PERGAMON

International Journal of Heat and Mass Transfer 42 (1999) 2935–2942

International Journal of HEAT and MASS TRANSFER

Heat transfer behavior of a temperature-dependent non-Newtonian fluid with Reiner–Rivlin model in a 2 : 1 rectangular duct

Sehyun Shin*, Hee-Hak Ahn, Young I. Cho[1], Chang-Hyun Sohn

School of Mechanical Engineering, Kyungpook National University, Taegu, Korea 702-701

Received 30 December 1997; in final form 29 September 1998

Abstract

The present study investigates the heat transfer enhancement mechanism observed with a non-Newtonian fluid having temperature-dependent viscosity in a 2 : 1 rectangular duct. The Reiner–Rivlin constitutive equation was used to model the non-Newtonian fluid characteristics. The H2 thermal boundary condition, corresponding to an axially-constant heat flux with a uniform heat flux at the top wall, was used. The local Nusselt numbers calculated for a polyacrylamide (Separan AP-273) solution showed significant heat transfer enhancements over those of a constant property fluid and gave excellent agreement with experimental results in both the regions of thermally developing and fully developed. The heat transfer enhancement results from an increased fluid mixing near the heated top wall, which is attributed to both the effects of the temperature-dependent viscosity and secondary flow induced by second normal stress difference. The present study concludes that the heat transfer enhancement of the viscoelastic fluid in a 2 : 1 rectangular duct is caused by the favorably combined effect of temperature-dependent viscosity and normal stress-induced secondary flow.

Nomenclature

$\bar{C}_p$ specific heat of fluid
$\bar{D}_h$ hydraulic diameter
Gz Graetz number, ($Re\ Pr\ \bar{D}_h/\bar{z}$)
$\bar{k}_f$ thermal conductivity of fluid
K fluid consistency index
n' flow behavior index for non-Newtonian fluids
Nu Nusselt number
Pr Prandtl number
$\bar{q}''$ heat flux
Re Reynolds number
Ra_q modified Rayleigh number, $Gr_q\ Pr$
T non-dimensional temperature, $(\bar{T}-\bar{T}_i)/(\bar{q}''\ \bar{D}_h/\bar{k}_f)$
V_x non-dimensional axial velocity, $(\bar{V}_x/\bar{V}_{avg})$
x non-dimensional axial distance, $(\bar{x}/\bar{D}_h\ Re\ Pr)$

Greek symbols

$\dot{\gamma}$ non-dimensional shear rate
$\bar{\eta}_{ref}$ (dimensional) reference viscosity (at inlet temperature of 20°C)
η non-dimensional viscosity, $\bar{\eta}/\bar{\eta}_{ref}$
η_0 zero-shear rate viscosity
λ characteristic time in equation (4)
ξ constant Deborah number-variation parameter in equation (4)
ζ constant viscosity-variation parameter in equation (4)

Superscript

$\bar{}$ dimensional

Subscripts

b bulk
CPF constant-property fluid
i inlet
w wall

* Corresponding author. Tel.: +82-53-950-6570; fax: +82-53-956-7907; e-mail: shins@bh.kyungpook.ac.kr

[1] Department of MEM, Drexel University, Philadelphia, PA, U.S.A.

0017–9310/99/$ - see front matter
PII: S0017–9310(98)00358–5

1. Introduction

Understanding non-Newtonian fluid flows and heat transfer behavior becomes increasingly important as the application of non-Newtonian fluids perpetuates through various industries, including polymer processing and electronic packaging. However, when one deals with a practical engineering problem consisting of a non-Newtonian fluid, it is not easy to estimate the heat transfer even in a simple geometry such as a rectangular duct. The reason is that the viscosity of non-Newtonian liquids varies with both shear rate and temperature, a phenomenon which significantly influences the velocity and temperature profiles. Consequently, the heat transfer and friction coefficients differ from those obtained with a constant-property fluid, whose viscosity is independent of shear rate and temperature.

Hartnett and his coworkers [1–3] showed significant laminar heat transfer enhancements with non-Newtonian fluids in rectangular ducts, an interesting phenomenon that had never been observed in a circular pipe flow. The physical mechanism of the heat transfer enhancement for the non-Newtonian fluids in the rectangular duct has not been clearly understood. Several researchers investigated the enhancement mechanism with experimental and numerical studies, which could be divided into two groups: one focuses on the temperature-dependent viscosity and the other is attributed to the secondary flow induced by the second normal stress difference of non-Newtonian viscoelastic fluids.

Among the first group, Shin and Cho [4, 5] estimated the laminar heat transfer of a polyacrylamide (Separan AP-273) solution by considering both temperature-dependent and shear-thinning viscosity. They reported 70–200% heat transfer enhancements over those of a constant-property fluid. Chang et al. [6] considered both temperature-dependent shear thinning viscosity and an axially developing secondary flow associated with the distortion of axial velocity. However, the value of Nusselt numbers calculated by both Shin and Cho [4] and Chang et al. [6] were smaller than those experimental results with the polyacrylamide solution reported by Xie and Hartnett [1]. Recently, Shin [7] considered the effect of both the shear rate-dependent thermal conductivity and temperature-dependent shear thinning viscosity of the polyacrylamide solution [8] on the laminar heat transfer behavior in a pipe flow. He found a 5–7% heat transfer enhancement over those of temperature-dependent shear thinning viscosity fluids.

Among the second group, Gao and Hartnett [9–10] investigated the effect of secondary flows for non-Newtonian viscoelastic fluids on the fully developed laminar heat transfer characteristics in a rectangular duct. They applied the Reiner–Rivlin constitutive equation with finite values of the second normal stress coefficient and found that the secondary flow resulted in a significant heat transfer enhancement, especially in rectangular ducts with aspect ratios of 0.5 and 1.0. However, the local Nusselt numbers numerically calculated with the Reiner–Rivlin equation were still smaller than those experimental results by Xie and Hartnett [1].

It was speculated that the heat transfer results reported by Xie and Hartnett [1] included the effects of both a temperature-dependent non-Newtonian viscosity and a normal stress-induced secondary flow. Hence, the objective of the present paper was to investigate the combined effect of the temperature-dependent non-Newtonian viscosity and the secondary flow induced by the second normal stress difference for a non-Newtonian viscoelastic fluid on the laminar heat transfer behavior in a top wall heated, 2 : 1 rectangular duct.

2. Problem description and assumptions

Figure 1 shows a schematic diagram of the system under consideration. Fluid entered the duct with a fully-developed parabolic velocity profile and a uniform temperature, Ti. The present study adopted the H2 thermal boundary condition corresponding to an axially constant heat flux with a uniform heat flux at the top wall. In order to delineate the effect of the buoyancy-induced secondary flow in the rectangular duct, the top wall was heated and other three walls were adiabatic.

The non-dimensional forms of the conservation equations of mass, momentum, and energy for a thermally-developing flow in a rectangular duct are given as follows:

Continuity:

$$\frac{\partial u_i}{\partial x_i} = 0 \tag{1}$$

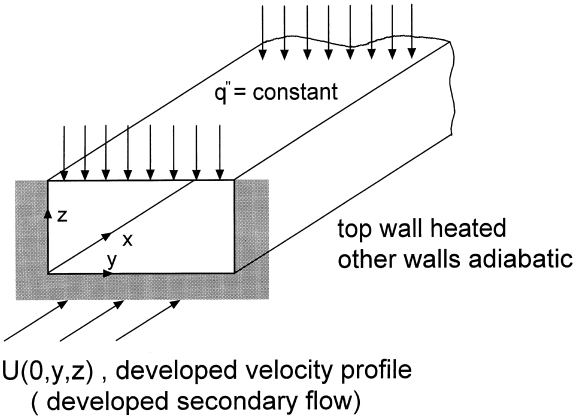

Fig. 1. Sketch of the cross-section of a 2 : 1 rectangular duct with hydrodynamic and thermal boundary conditions.

Axial momentum:

$$\frac{\partial(\rho u_j u_k)}{\partial x_k} = -\frac{\partial P}{\partial x_j} + \frac{1}{Re^+}\left(\frac{\partial \tau_{jk}}{\partial x_k}\right) \tag{2}$$

Energy:

$$\frac{\partial(\rho c T u_j)}{\partial x_j} = \frac{1}{Pr^+ Re^+}\left[\frac{\partial}{\partial x_j}\left(k\frac{\partial T}{\partial x_j}\right)\right] \tag{3}$$

The temperature-dependent Carreau model [5] was used in the present study to consider both the shear-thinning and the temperature-dependent viscosity of a non-Newtonian fluid.

$$[\eta(\dot\gamma, T)-\eta_\infty]/[\eta_{0\mathrm{ref}}10^{(\zeta T)}-\eta_\infty] = [1+(De10^{\xi T}\dot\gamma)^2]^{(n'-1)/2} \tag{4}$$

In the above equation, De is the Deborah number ($\lambda V_{avg}/D_h$), ξ is a constant accounting for the temperature dependence of time constant (λ), and ζ represents the slope of η_0 vs T curve. The slope becomes negative for heating case and positive for cooling case. T is a dimensionless temperature introduced for the H2 boundary condition, defined as

$$T = \frac{(\bar T - \bar T_i)}{(\bar q'' \bar D_h/\bar k_f)} \tag{5}$$

Equation (4) considers the effects of temperature on the apparent viscosity and the time constant of a non-Newtonian fluid.

Non-Newtonian viscoelastic fluids exhibit normal stress differences under shear flow conditions. Green and Rivlin [12] reported the existence of a secondary flow in an elliptical duct flow. They used the Reiner–Rivlin constitutive equation which was of the following form:

$$\sigma_{ij} = -p\delta_{ij} + \eta d_{ij} + \alpha_2 d_{ik} d_{kj} \tag{6}$$

where

$$d_{ij} = \left(\frac{\partial u_i}{\partial x_j} + \frac{\partial u_j}{\partial x_i}\right) \tag{7}$$

For the purpose of computing the secondary flow in a non-circular duct, the Reiner–Rivlin constitutive equation was known to be as good as the CEF equation [11]. Therefore, the present study chose the Reiner–Rivlin constitutive equation to model the fluid motion of a non-Newtonian viscoelastic fluid in a rectangular duct.

For the Reiner–Rivlin constitutive equation, the second normal stress difference becomes zero for a purely-viscous non-Newtonian fluid. The (dimensionless) second normal stress difference coefficient, α_2, is non-dimensionalized as follows:

$$\alpha_2 = (Re^+/D_h\rho_{ref})\bar\alpha_2 \tag{8}$$

Gao and Hartnett [9] applied the Reiner–Rivlin constitutive equation to calculate flow and heat transfer behavior of polyacrylamide solutions with various α_2. Using the values of α_2 ranging from 0.003–0.0103, they obtained the heat transfer enhancement results which agreed well with the experimental results reported by Hartnett and Xie [13]. Figure 2 shows a typical example of the secondary flow field in a fully developed laminar flow calculated using the Reiner–Rivlin constitutive equation with $\alpha_2 = 0.0031$ in a 2 : 1 rectangular duct.

Since detailed descriptions of the boundary conditions and the solution methodology have been given elsewhere [4, 14], only a brief summary is given below. The no-slip boundary condition is applied along the periphery of the duct for velocity components. The constant heat flux boundary condition is applied only on the top wall of the rectangular duct. The other three walls are assumed to be adiabatic.

Solutions to the problem defined by the foregoing equations were obtained numerically by a SIMPLE-C algorithm with finite volume procedures. A QUICK scheme proposed by Hayase et al. [15] was employed for the convective term in the energy equation for all interior nodal points while a third-order accurate difference scheme was employed at the boundary surfaces. For near-boundary control volumes, there was no need for a special discretization equation since the boundary condition data could be directly employed at the boundary face.

Convergence for the present calculation was monitored by examining how well the discretization equation was satisfied by the current values of the dependent variables, ϕ. Since the order of magnitude of the secondary flow was 10^{-3} of the main flow in the present analysis, it was necessary to keep the accuracy for the secondary flow calculation within 0.01%. Thus, the convergence criteria for the present calculation, which was the absolute difference of dependent variables at each iteration, was set to be less than 10^{-7}.

$$|\phi^{n,\mathrm{step}} - \phi^{n-1,\mathrm{step}}| < 10^{-7} \tag{9}$$

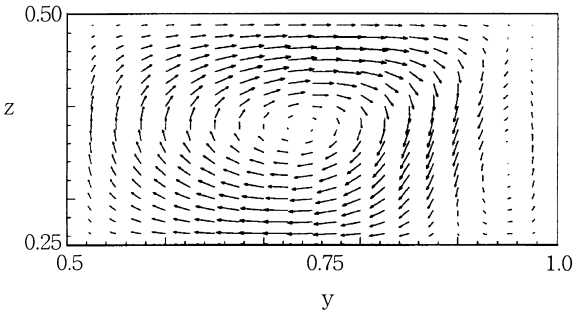

Fig. 2. Secondary flows calculated for a Reiner–Rivlin fluid ($\alpha_2 = 0.0031$) in a fully developed laminar flow through a 2 : 1 rectangular duct. The upper right quadrant of the duct is shown. $Re^+ = 96$, $n = 0.643$.

3. Results and discussion

The present numerical study used the viscosity data of an aqueous polyacrylamide (Separan AP-273, 1000 wppm) solution reported by Shin and Cho [5]. The viscosity data shown in Fig. 3 were fitted using equation (4), and the maximum deviation between the measured viscosities and the predicted values from equation (4) was 4%. Also, the present numerical study used the Reiner–Rivlin constitutive equation to represent the second normal stress difference for the polyacrylamide solution.

Prior to reporting the present numerical results, the appropriate grid size for a constant-property fluid was assessed—a case in which well-established values of fRe_{ref} were available. On a uniform grid, grid sizes were varied, and the continuity and momentum equations were solved. The exact analytical value of fRe_{ref} in the fully-developed flow of a 2 : 1 rectangular duct was 15.54806; Shah and London's value was 15.55733; the corresponding value from the present study with 62×62 uniform grid was 15.52953. The values of fRe_{ref} became independent of grid sizes beyond 41×41. Hence, the present study used the results calculated from the 41×41 uniform grid size.

Figure 4(a) shows two sets of dimensionless temperature profiles on the mid-plane (i.e., at $y = 0.5$) calculated for the polyacrylamide solution and a constant property fluid (CPF) at two axial locations. Note that $z = 0.5$ refers to the heated top wall whereas $z = 0$ refers to the unheated bottom wall. Near the inlet (i.e., at $x = 0.005$), there was not much difference between the two temperature profiles of the polyacrylamide solution and CPF. However, in the middle of the thermally-developing region (i.e., at $x = 0.05$), the temperature near the heated top wall for the polyacrylamide solution was much less than that for CPF. This phenomenon was previously reported by Shin and Cho [4]. They attributed it to an increased velocity gradient near the heated top wall, which resulted in the heat transfer enhancement and subsequent reduction of wall temperature.

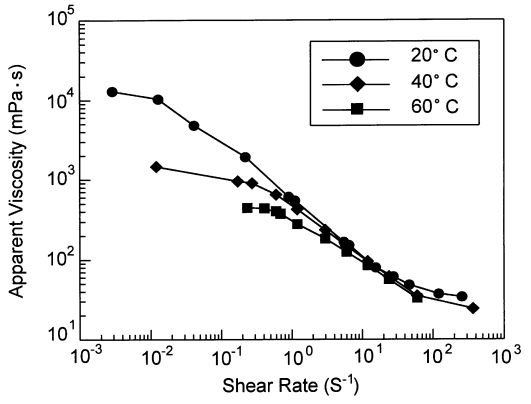

Fig. 3. Variation of the viscosity of polyacrylamide solution (Separan AP-273, 1000 wppm) with shear rate at three different temperatures.

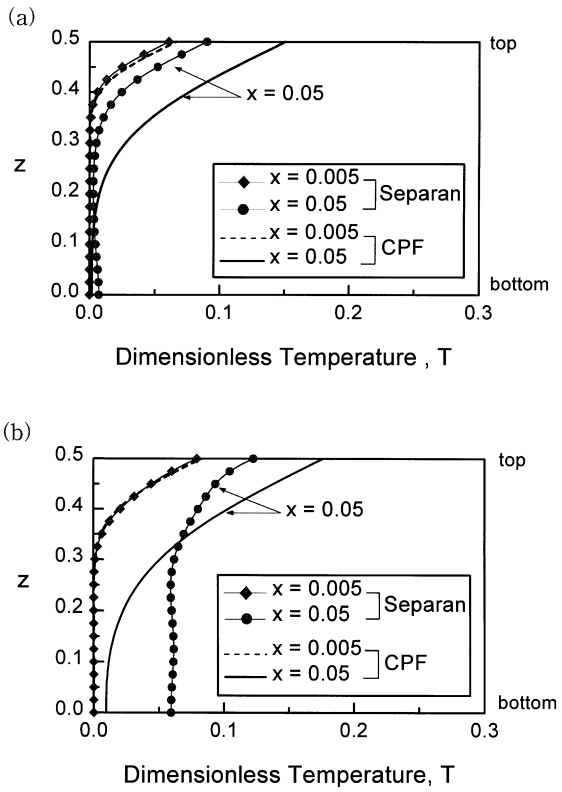

Fig. 4. Dimensionless temperature profiles for polyacrylamide solution and CPF (constant-property fluid) along the vertical direction (z) in a 2 : 1 rectangular duct with heated top wall. (a) $y = 0.5$ (mid-plane), and (b) $y = 0.1$ (near the side wall).

Figure 4(b) shows two sets of dimensionless temperature profiles on a plane near the side wall (i.e., at $y = 0.1$). At $x = 0.05$, the temperature calculated for the polyacrylamide solution near the unheated bottom wall was much higher than that for CPF. This phenomenon can be attributed to an efficient fluid mixing caused by the secondary flow in the 2 : 1 rectangular duct for polyacrylamide solution.

In order to delineate the combined effect of variable viscosity and secondary flow on velocity profiles, Fig. 5 shows the velocity profiles calculated at two different axial locations (i.e., at $x = 0$ and 0.05). The velocity profile shown in Fig. 5(a) (i.e., at $x = 0$) represents the fully-developed velocity profile for CPF. Compared to the velocity profiles in Fig. 5(a), those given in Fig. 5(b) show a much steeper velocity gradient near the heated top wall (i.e., at $z = 0.5$). The fact implies that the reduction of

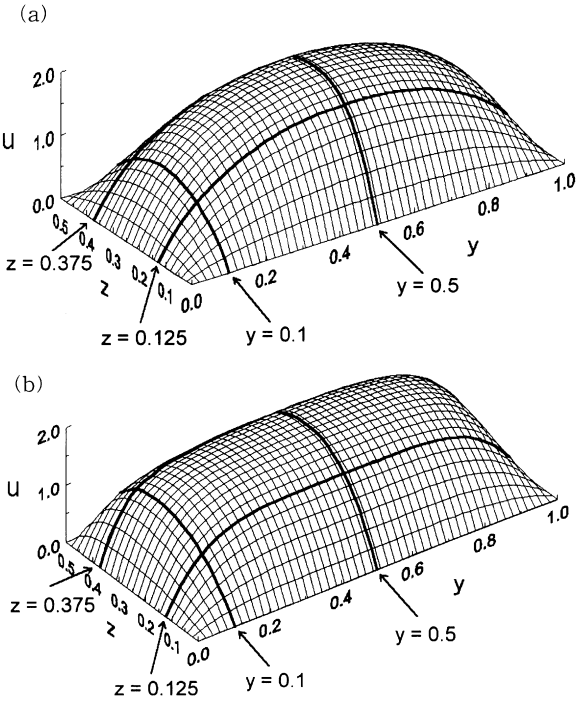

Fig. 5. Dimensionless axial velocity profiles calculated for polyacrylamide solution at two different axial locations in a 2:1 rectangular duct. (a) $x = 0$ (inlet), and (b) $x = 0.05$. $z = 0.5$ represents heated top wall.

the viscosity caused a much steeper velocity gradient near the heated wall with increasing axial distance for the polyacrylamide solution than for the constant property fluid (CPF). Furthermore, the secondary flow may increase the distortion of velocity profiles associated with fluid mixing near the heated top wall.

The maximum velocity for the polyacrylamide solution at $y = 0.5$ was slightly smaller than that for CPF while the location of the maximum velocity was almost identical with that for CPF. Meanwhile, the velocity profile for the polyacrylamide solution at $y = 0.1$ was bigger than that for CPF, and the location of the maximum velocity was shifted upward. The combined effect of the variable viscosity and the secondary flow caused a lateral distortion of the axial velocity. At $z = 0.375$, the velocity profile became flat with the same magnitude of the center velocity along the axial distance. However, the velocity profile at $z = 0.125$ became flat with decreasing center velocity along the axial distance.

Figure 6 shows secondary flow patterns calculated at four different axial locations (i.e., at $x = 0.0$, 0.005, 0.02, and 0.05) at the right half cross section of the rectangular duct. The distortion of the axial velocity is believed to affect the secondary flow which is created by the second normal stress difference of the polyacrylamide solution. Of note is that when the normal stress difference was not considered in the constitutive equation, the secondary flows did not exist, confirming that the secondary flows were created by the normal stress difference of the polyacrylamide solution.

Figure 6(a) shows two symmetric vortices at $x = 0$ when the second normal stress difference of the polyacrylamide solution was considered. The magnitude of the secondary flow increased along the axial distance as shown in Figs 6(b)–(d). The upper cell of the secondary flow at $x = 0$ transforms to one large cell at $x = 0.05$. The transformation of the two cells into one large cell was due to an increasing top wall velocity caused by the reduction of viscosity near the heated top wall.

Subsequently, the secondary flow cell at the top wall continues to grow, resulting in a large single cell at $x = 0.05$. On the other hand, when the temperature-dependent viscosity was not considered but the second normal stress difference of the polyacrylamide solution was considered, the two cells observed at $x = 0.0$ continued to exist throughout the entire axial distance.

Figure 7(a) and (b) show temperature profiles for CPF and the polyacrylamide solution at $x = 0.05$, respectively. The temperature profile for CPF shows a gradual decrease from the top wall (i.e., $z = 0.5$) to the bottom wall (i.e., $z = 0$), while the temperature did not vary much along the y-direction. The temperature profile for the polyacrylamide solution shown in Fig. 7(b) is much more complex than that for CPF. This is mainly due to the distortion of the flow associated with the temperature-dependent viscosity and the secondary flow caused by the second normal stress difference. Temperature near the heated top wall for the polyacrylamide solution was much smaller than that for CPF. For example, the temperature at the center of the top wall for the polyacrylamide solution was 0.09 whereas that for CPF was 0.151. However, the temperature at the corner of the bottom wall was much higher than that for CPF, which reflects the direction of the secondary flow as shown in Fig. 6(d).

Figure 8 shows the temperature difference between wall and bulk, $\Delta T_{\text{wall–bulk}}$, along the axial direction for both the polyacrylamide solution and CPF. It is of note that a thermally-fully-developed flow is obtained when $\Delta T_{\text{wall–bulk}}$ reaches a plateau value. The results in Fig. 8 indicate that the thermal entrance length, L_{th}^{+}, for CPF was approximately 0.2–0.3 in the top-wall-heated rectangular duct. The polyacrylamide solution yielded much shorter thermal entrance lengths ($L_{\text{th}}^{+} = 0.05$–0.07) than for CPF due to the temperature-dependent viscosity and secondary flow.

In order to examine the combined effect of the variable viscosity and the secondary flow on the laminar heat transfer for the polyacrylamide solution, local Nusselt numbers are shown at two different modified Rayleigh numbers (Ra_{q}) in Fig. 9. The local Nusselt numbers cal-

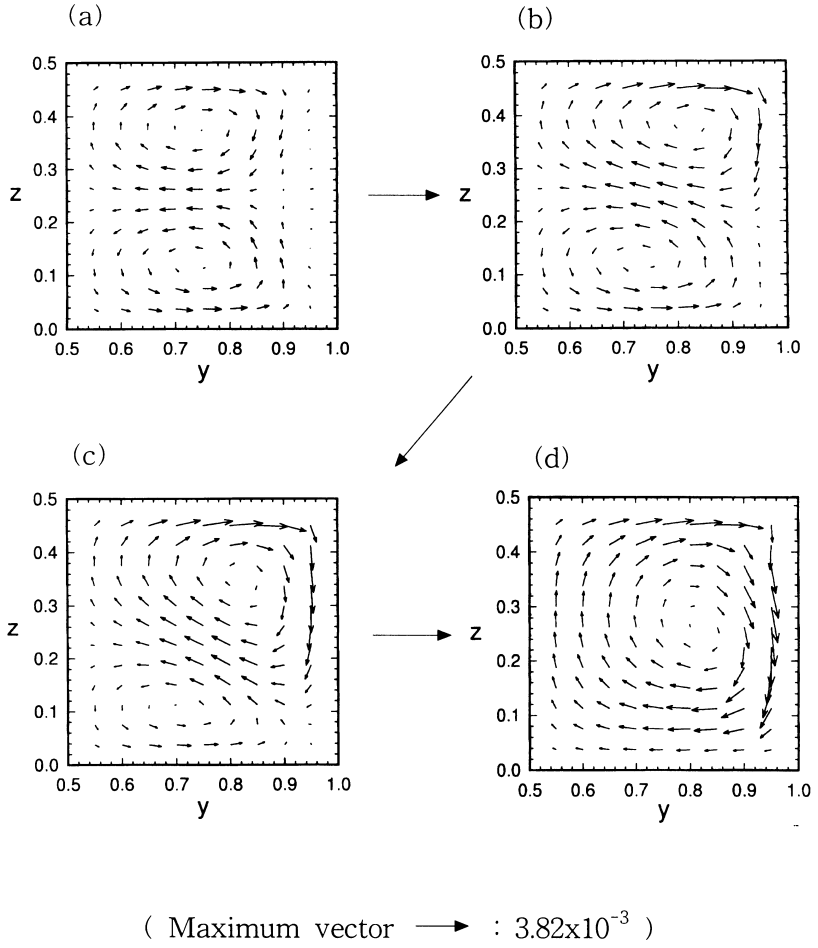

Fig. 6. Secondary flows calculated for polyacrylamide solution at four different axial locations (i.e., at $x = 0$, 0.005, 0.02, and 0.05) in a 2 : 1 rectangular duct with heated top wall.

culated in the present study gave an excellent agreement with experiments reported by Xie and Hartnett [1]. In the thermally-fully-developed region, the present calculation for CPF yielded a Nusselt number of 3.56, which is almost identical to the analytical value in a pipe flow ($Nu = 3.54$). The Nusselt numbers for the polyacrylamide solution increased by 200–300% above the value obtained with CPF.

The laminar heat transfer enhancement with the polyacrylamide solution is believed to occur because of the secondary flow as well as the decrease in the viscosity near the heated top wall. The latter brings out a significant increase in velocity gradients and subsequent change in the secondary flow pattern, rendering an efficient fluid mixing and an overall increase in the local heat convection performance.

4. Conclusion

The present study examined the combined effect of the temperature-dependent shear-thinning viscosity and the secondary flow caused by the second normal stress difference on the laminar heat transfer behavior in a top-wall-heated 2 : 1 rectangular duct. The local Nusselt numbers calculated for the polyacrylamide solution gave excellent agreement with the experimental results [3], showing 200–300% enhancement over those of a constant-property fluid. The heat transfer enhancement observed with the polyacrylamide solution was due to the combined effect of temperature-dependent viscosity and secondary flow. Hence, it is concluded that the main mechanism of the heat transfer enhancement for the polyacrylamide solution was composed with two: one was the

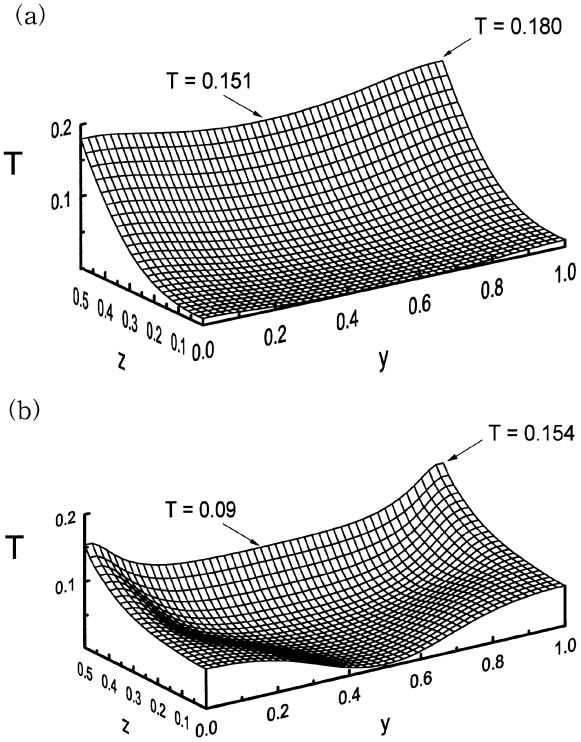

Fig. 7. Dimensionless temperature profiles calculated for (a) CPF and (b) polyacrylamide solution at $x = 0.05$ in a 2 : 1 rectangular duct with heated top wall. For the polyacrylamide solution, both temperature-dependent non-Newtonian viscosity and secondary flow caused by the second normal stress difference were considered. $z = 0.5$ represents heated top wall.

temperature-dependent non-Newtonian viscosity and the other was the secondary flow generated by the second normal stress difference in the 2 : 1 rectangular duct.

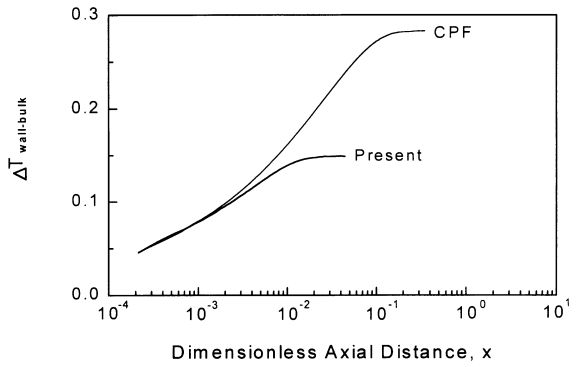

Fig. 8. Temperature difference between wall and bulk, $\Delta T_{wall-bulk}$, along the dimensionless axial distance calculated for CPF and polyacrylamide solution in a 2 : 1 rectangular duct with heated top wall.

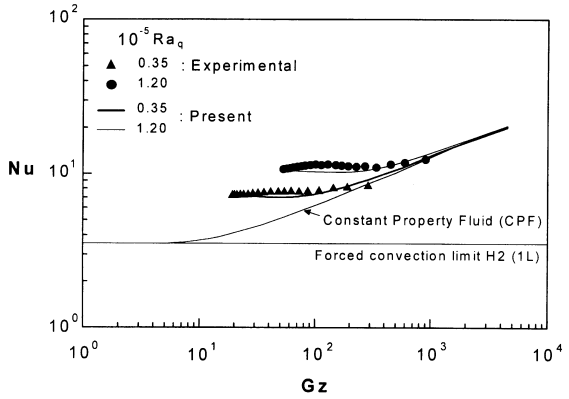

Fig. 9. Comparison of the present numerical laminar heat transfer results calculated for both CPF and polyacrylamide solution with experimental results reported by Xie and Hartnett [1] in a 2 : 1 rectangular duct with heated top wall.

References

[1] C. Xie, J.P. Hartnett, Influence of rheology on laminar heat transfer to viscoelastic fluids, Ind. Engng. Chem. Res. 31 (1992) 727–732.
[2] J.P. Hartnett, Viscoelastic fluids: experimental challenges, Experimental Heat Transfer 5 (1991) 621–626.
[3] J.P. Hartnett, M. Kostic, Heat transfer to a viscoelastic fluid in laminar flow through a rectangular channel, Int. J. Heat Mass Transfer 28 (1985) 1147–1155.
[4] S. Shin, Y.I. Cho, Laminar heat transfer in a rectangular duct with a non-Newtonian fluid with temperature dependent viscosity, Int. J. Heat Mass Transfer 37 (1) (1994) 19–30.
[5] S. Shin, Y. Cho, Temperature effect on the viscosity of an aqueous polyacrylamide solution, Int. Comm. Heat Mass Transfer 20 (1993) 831–844.
[6] P.Y. Chang, F.C. Chou, C.W. Tung, Heat transfer mechanism for Newtonian and non-Newtonian fluids in 2 : 1 rectangular ducts, Int. J. Heat Mass Transfer 41 (1998) 3841–3856.
[7] S. Shin, The effect of the shear rate-dependent thermal conductivity of non-Newtonian fluids on the heat transfer in a pipe flow, Int. Comm. Heat Mass Transfer 23 (1996) 665–678.
[8] D.Y. Lee, Thermal conductivity measurements of non-Newtonian fluids in a shear field, Ph.D. Thesis, State University of New York at Stony Brook (1995).
[9] S.X. Gao, J.P. Hartnett, Steady flow of non-Newtonian fluids through rectangular ducts, Int. Comm. Heat Mass Transfer 20 (1993) 197–210.
[10] S.X. Gao, J.P. Hartnett, Heat transfer behavior of Reiner–Rivlin fluids in rectangular ducts, Int. J. Heat Mass Transfer 39 (6) (1996) 1317–1324.
[11] B. Gervang, P.S. Larsen, Secondary flows in straight ducts of rectangular cross section, J. non-Newtonian Fluid Mechanics 39 (1991) 217–237.

[12] A.E. Green, R.S. Rivlin, Steady flow of non-Newtonian fluids through tubes, Q. Appl. Math. 14 (3) (1956) 299–308.
[13] J.P. Hartnett, C.B. Xie, Symposium series No. 269 (1989) 454–459.
[14] S. Shin, Y.I. Cho, W.K. Gingrich, W. Shyy, Numerical study of laminar heat transfer with temperature dependent viscosity in a 2 : 1 rectangular duct, Int. J. Heat Mass Transfer 36 (1992) 641–648.
[15] T. Hayase, J.A.C. Humphrey, R. Greif, A consistently formulated QUICK scheme for fast and stable convergence using finite-volume iterative calculation procedures, J. Computational Physics 98 (1992) 108–118.